HHS Public Access

Author manuscript

Nat Neurosci. Author manuscript; available in PMC 2015 May 01.

Published in final edited form as:

Nat Neurosci. 2014 November ; 17(11): 1583–1590. doi:10.1038/nn.3822.

Social learning and amygdala disruptions in Nf1 mice are rescued by blocking p21-activated kinase

Andrei I. Molosh[1,2,*], **Philip L. Johnson**[1,2,4,*], **John P. Spence**[1,3], **David Arendt**[1], **Lauren M. Federici**[2,3,4], **Cristian Bernabe**[4], **Steven P. Janasik**[1], **Zaneer M. Segu**[10], **Rajesh Khanna**[2,5], **Chirayu Goswami**[8], **Weiguo Zhu**[2,5], **Su-Jung Park**[6], **Lang Li**[8], **Yehia S. Mechref**[10], **D. Wade Clapp**[6,7], and **Anantha Shekhar**[1,2,5,9]

[1]Department of Psychiatry, Institute of Psychiatric Research, Indiana University School of Medicine, Indianapolis, IN 46202

[2]Stark Neurosciences Research Institute, Indiana University School of Medicine, Indianapolis, IN 46202

[3]Program in Medical Neurosciences, Indiana University School of Medicine, Indianapolis, IN 46202

[4]Department of Anatomy and Cell Biology, Indiana University School of Medicine, Indianapolis, IN 46202

[5]Department of Pharmacology and Toxicology, Indiana University School of Medicine, Indianapolis, IN 46202

[6]Department of Pediatrics, Indiana University School of Medicine, Indianapolis, IN 46202

[7]Department of Microbiology and Immunology, Indiana University School of Medicine, Indianapolis, IN 46202

[8]Center for Computational Biology and Bioinformatics, Indiana University School of Medicine, Indianapolis, IN 46202

[9]Indiana Clinical and Translational Sciences Institute, Indiana University School of Medicine, Indianapolis, IN 46202

Correspondence to: Anantha Shekhar, M.D., Ph.D., Indiana University School of Medicine, 410 W. 10th Street, Suite 1100, Indianapolis, IN 46202, Tel: 317-278-2874; Fax: 317-278-4821, ashekhar@iupui.edu.

*authors made equal contribution to this report

Authors contributions.

AIM, PLJ, JPS, DWC and AS formulated the hypotheses and designed the studies. SJP and DWC maintained colony and genotyped all mice. JPS and SPJ performed behavioral assays in Figure 1, and JPS in Figure 2. For Figure 1 and Supplemental Figure 3, western blots were performed by RK and WZ, and immunohistochemistry was performed by LMF and PLJ. AIM performed all electrophysiology experiments in Figure 3. For Table 1 and 4a-b and Supplemental Table 1, AIM micropunched BLA, and YM and ZMS conducted proteomics assay, and CG, LL and PLJ analyzed the data. Immunohistochemistry in Figure 4c-f was performed by LMF and PLJ. Stereotaxic surgeries and behavioral assays in Figure 5, were performed by DA and CB. Stereotaxic surgeries and immunohistochemistry in Supplemental Figure 2 was done by DA and PLJ. AIM and PLJ analyzed data, and created figures. AIM, PLJ, JPS, DWC and AS interpreted the data and collectively wrote the main draft of the article with all other authors contributing to the revisions and all have approved of the final version.

[10]Department of Chemistry, METACyt Biochemical Analysis Center, Indiana University, Bloomington, IN 47405

Abstract

Children with Neurofibromatosis type 1 (NF1) are increasingly recognized to have high prevalence of social difficulties and autism spectrum disorders (ASD). We demonstrated selective social learning deficit in mice with deletion of a single Nf1 gene (*Nf1*$^{+/-}$), along with greater activation of mitogen activated protein kinase pathway in neurons from amygdala and frontal cortex, structures relevant to social behaviors. The *Nf1*$^{+/-}$ mice showed aberrant amygdala glutamate/GABA neurotransmission; deficits in long-term potentiation; and specific disruptions in expression of two proteins associated with glutamate and GABA neurotransmission: a disintegrin and metalloprotease domain 22 (ADAM22) and heat shock protein 70 (HSP70), respectively. All of these amygdala disruptions were normalized by co-deletion of p21 protein-activated kinase (Pak1) gene. We also rescued the social behavior deficits in *Nf1*$^{+/-}$ mice with pharmacological blockade of Pak1 directly in the amygdala. These findings provide novel insights and therapeutic targets for NF1 and ASD patients.

Introduction

Affecting roughly 1 in 3000 children, NF1 is one of the most common single gene disorders, resulting in the development of complex tumors known as neurofibromas with significant cognitive and learning disabilities[1,2]. A number of studies demonstrate deficits in social information processing and social behaviors in over 50% of NF1 patients[3–6], with 20–30% reaching the severity of clinical diagnosis of autism spectrum disorders (ASD)[7–9]. Further analyses of these social deficits in NF1 patients suggest that there are problems in facial emotional recognition (especially fear), a task that is specifically linked to human amygdala function[6,10].

Thus, NF1 mutation presents an important single gene disruption model that could provide insights into the molecular mechanisms for social learning deficits and pathophysiology of ASD. Social learning is the product of complex interactions between multiple structures in the CNS, particularly the amygdala, striatum, hippocampus, fusiform area and frontal cortex[11–13]. Using homologous recombination to disrupt the murine homologue of *NF1* (*Nf1*), loss of a single *Nf1* allele in mice (*Nf1*$^{+/-}$ mice) reduces neurofibromin levels in multiple organs, and recapitulating the phenotypes of the human condition[14]. Specifically, it causes deficits in some forms of spatial learning, as well as disrupted hippocampal long-term potentiation (LTP)[15,16]. In addition to the hippocampus, *Nf1*$^{+/-}$ mice also show significant reductions in neurofibromin levels in the amygdala and frontal cortex, CNS sites critical for social behaviors and emotional regulation. Therefore, the present study was conducted to test if *Nf1*$^{+/-}$ mice demonstrate disruptions in social behaviors and to elucidate cellular or molecular changes in CNS sites associated with social behaviors.

Results

To determine whether *Nf1*$^{+/-}$ mice demonstrate disrupted social learning, we used a well validated three chamber social memory test[17]. On initial exposure to the testing apparatus, both *WT* and *Nf1*$^{+/-}$ strains spent significantly more time interacting with an unfamiliar mouse over an inanimate object [n=12/12; side preference effect $F_{1,22} = 105.8$, $p < 0.001$, but no *Nf1*$^{+/-}$ interaction, $F_{1,22} = 0.9$, $p = 0.358$, Fig. 1a], demonstrating that the *Nf1*$^{+/-}$ genotype does not affect conspecific social cue recognition in mice (labeled baseline social behavior). After a 10 min interval, mice were retested with a choice between a novel mouse and the previous familiar mouse to assess their short-term social memory[18]. Both *WT* and *Nf1*$^{+/-}$ genotypes spent significantly more time with the new mouse [n=12/12, side preference effect $F_{1,22} = 105.8$, $p < 0.001$, but no *Nf1*$^{+/-}$ interaction, $F_{1,22} = 0.4$, $p = 0.554$; Fig. 1b], suggesting that *Nf1*$^{+/-}$ mice show normal ability to discriminate and immediately recall social cues. However, when presented with yet another novel mouse and the previously "familiar" mouse 24 hours later, the *Nf1*$^{+/-}$ mice did not show increased exploration of the novel mouse compared to the "familiar" mouse, whereas the *WT* mice showed robust preference for the novel mouse [n=12/11, side preference effect $F_{1,21} = 9.9$, $p = 0.005$, and a *Nf1*$^{+/-}$ interaction, $F_{1,21} = 5.3$, $p = 0.032$; Fig. 1c–d]. These results indicate that *Nf1*$^{+/-}$ mice, while showing normal immediate social discrimination at baseline, were unable to retain or recall the social memory and discriminate between familiar and unfamiliar social cues following a 24-hour delay.

To confirm if this deficit was selective for social learning or generalized to other amygdala-cortical circuits, we also tested the performance of *Nf1*$^{+/-}$ mice in other novelty and emotional learning paradigms. We confirmed that compared to *WT*, *Nf1*$^{+/-}$ mice did not demonstrate deficits in learning in a novel object recognition test [n=5/5, object preference effect $F_{1,8} = 8.9$, $p = 0.017$, but no *Nf1*$^{+/-}$interaction, Fig. 1e], or avoidance learning in passive avoidance test [n=9,6, avoidance effect $F_{1,13} = 16.1$, $p = 0.001$, but no *Nf1*$^{+/-}$ interaction, Fig. 1f]. Ability to demonstrate innate avoidance of a fear stimulus 24 hours later was also tested by utilizing the elevated plus-maze as previously described[19]. When tested 24 hours later, both genotypes showed similar increases in the avoidance of the open arms, suggesting normal retention of memory for aversive cues and avoidance in both genotypes [n=12/12, respectively, a day effect for duration $F_{1,22} = 10.1$, $p = 0.003$, Fig. 1g, and entries $F_{1,22} = 11.5$, $p = 0.003$, Fig. 1h in open arms but no *Nf1*$^{+/-}$ interactions]. Similarly, utilizing the Porsolt forced swim test, we measured the development of behavioral despair 24 hours later in the *Nf1*$^{+/-}$ mice. The *WT* and *Nf1*$^{+/-}$ mice both showed normal learning in the forced swim test [n=12/12, day effect $F_{1,22} = 5.1$, $p = 0.034$, but no *Nf1*$^{+/-}$ interaction, Fig. 1i]. The *Nf1*$^{+/-}$ mice were also tested for differences in the ability to discriminate olfactory cues, another possible confound that could result in mice showing poor social learning. In a standardized olfactory habituation test both *WT* and *Nf1*$^{+/-}$ mice demonstrated similar learning [n=6/6, Water, test effect $F_{2,20} = 15.2$, $p < 0.001$, Almond, test effect $F_{2,20} = 7.4$, $p = 0.004$, and, novel mouse, test effect $F_{2,20} = 37.1$, $p < 0.001$, but no *Nf1*$^{+/-}$ interactions, Fig. 1j]. Thus, *Nf1*$^{+/-}$ mice appeared to have selective and circumscribed deficits in long-term retention of social information.

The *NF1* gene encodes neurofibromin, which negatively regulates Ras GTPase activation (see Suppl. Fig. 1a for hypothetical illustration). Mutation at the *Nf1* locus increases the output of MAPK and PI3K signal transduction from the cellular membrane to the nucleus resulting in the hyperactivation of the products of its downstream pathways such as phosphorylated ERK[20,21]. Therefore, we first tested whether neurons cultured from $Nf1^{+/-}$ mice would display a similar hyperactivation of MAPK following growth factor stimulation. Application of recombinant murine Stem Cell Factor (SCF; 10 ng/ml) increased the pERK1/2 levels to significantly greater degree in frontal cortical neurons cultured from $Nf1^{+/-}$ mice when compared to those cultured from *WT* mice (n=3/3, pERK/total ERK post stimulation, $t_4 = -4.0$, $p = 0.017$, Fig. 1k). Applying SCF to amygdala cultures $Nf1^{+/-}$ mice increased pERK1/2 by ~100% compared to a ~ 50% increase in *WT* mice (n=4/4, pERK/tERK post stimulation, $t_6 = -1.8$, $p = 0.114$, Fig. 1k). To complement these *in vitro* findings, we also assessed pERK immunostaining in subregions of the amygdala in WT and $Nf1^{+/-}$ mice following exposure to a novel mouse. Compared to *WT* mice, $Nf1^{+/-}$ mice had increased numbers of pERK immunoreactive cells in the basolateral amygdala [BLA: $t_9 = 3.2$, $p = 0.010$], but not medial amygdala (n=5/6, $t_9 = 1.2$, $p = 0.262$, Fig. 1l), further demonstrating hyperactivity of MAPK pathways in neurons responding to a social cue.

PAK1 is a downstream effector regulated by the Rho family of GTPases and positively regulates MAPK activation, and deletion of Pak1 gene ($Pak1^{-/-}$ mice) could potentially normalize the hyperactivation of MAPK pathways seen in the $Nf1^{+/-}$ mice as previously demonstrated in macrophages[22] (see Suppl. Fig. 1a). In order to confirm that this approach could normalize social learning deficits in $Nf1^{+/-}$ mice, we tested if genetic intercross ($Nf1^{+/-}/Pak1^{-/-}$) would restore the learning deficits seen in $Nf1^{+/-}$ mice. We found that $Nf1^{+/-}$, $Nf1^{+/-}/Pak1^{-/-}$, and $Pak1^{-/-}$ strains showed no differences in baseline social preference (n=12/11/6, side preference effect $F_{1,26} = 100.5$, $p < 0.001$, but no genotype interaction, Fig. 2a) or short-term social learning (n=12/11/6, side preference effect $F_{1,26} = 32.7$, $p < 0.001$, but no genotype interaction, Fig. 2b]. As before, deficits were seen in $Nf1^{+/-}$ mice in long-term social learning, but importantly, co-deletion of $Pak1^{-/-}$ in $Nf1^{+/-}$ mice ($Nf1^{+/-}/Pak1^{-/-}$ mice) clearly restored this learning deficit [n=12/11/6, side preference effect $F_{1,26} = 7.5$, $p = 0.011$, and a genotype x side preference interaction that approached significance $F_{1,26} = 3.3$, $p = 0.054$, a Fisher's exact test determined that $Nf1^{+/-}/Pak1^{-/-}$ mice show a greater novel mouse preference (= 10 sec criteria) than $Nf1^{+/-}$ mice p = 0.036, Fig. 2c–d]. Similar to our previous results with $Nf1^{+/-}$ mice, we detected no differences in anxiety (n=12/11/6, day effect $F_{2,26} = 36.6$, $p < 0.001$, but no genotype interaction, Fig. 2e), or olfaction (n=12/11/6, test 1–3 effects were noted for water, $F_{2,30} = 12.2$, $p < 0.001$, almond, $F_{2,30} = 23.2$, $p < 0.001$, novel mouse, $F_{2,30} = 26.3$, $p < 0.001$, but not genotype interactions; Fig. 2g) between the $Nf1^{+/-}$ and $Nf1^{+/-}/Pak1^{-/-}$ mice. Although despair-associated behaviors are not different between *WT* and $Nf1^{+/-}$ mice (Fig. 1i), compared to $Nf1^{+/-}$ mice the $Nf1^{+/-}/Pak1^{-/-}$, and $Pak1^{-/-}$ *mice* had reduced despair associated immobility (n=12/11/6, genotype effect, $F_{2,26} = 6.9$, $p = 0.004$; day effect $F_{2,26} = 9.2$, $p = 0.005$; but no genotype interaction, Fig. 2f). Overall, these results determined that constitutive *Pak1* co-deletion could rescue the social learning deficits in $Nf1^{+/-}$ mice.

Since the amygdala is important in social learning[11–13] and we observed hyperactivity of MAPK pathways in BLA neurons of *Nf1*$^{+/-}$ mice post novel mouse exposure (Fig. 1l), we next assessed functional changes in the amygdala networks in *WT*, *Nf1*$^{+/-}$, *Nf1*$^{+/-}$/*Pak1*$^{-/-}$ and *Pak1*$^{-/-}$ mice. Using whole-cell patch-clamp from BLA principal neurons we studied spontaneous excitatory and inhibitory postsynaptic currents (sEPSCs and sIPSCs, respectively). While pyramidal neurons of the BLA from *Nf1*$^{+/-}$ mice exhibited no differences in the amplitudes of either sIPSC [n=4/4/3/3 mice/genotype and n=11/11/14/14 cells patched/genotype, no Nf1$^{+/-}$ x Pak1$^{-/-}$ interaction, $F_{1,46} = 0.1$, p = 0.77, Fig. 3a,b] or miniature IPSCs (mIPSCs) [no *Nf1*$^{+/-}$ x *Pak1*$^{-/-}$ interaction, $F_{1,46} = 0.3$, $p = 0.59$, Fig. 3a,b], they did show significant increases in the frequencies of both sIPSC [*Nf1*$^{+/-}$ x *Pak1*$^{-/-}$ interaction, $F_{1,46} = 6.11$, $p = 0.017$, Fig. 3a,c] and mIPSC [*Nf1*$^{+/-}$ x *Pak1*$^{-/-}$ interaction, $F_{1,46} = 9.21$, $p = 0.004$, Fig. 3a,c] compared to *WT* mice. Furthermore, co-deletion of Pak1 completely normalized the increase in frequency, without affecting the amplitude of sIPSC and mIPSC in the amygdala neurons [Fig. 3a–c], confirming that Pak1 deletion also restores the increased BLA network inhibitory activity induced by *Nf1* mutation.

Next, analysis of both sEPSCs and mEPSCs from pyramidal neurons in the BLA of *Nf1*$^{+/-}$ mice showed significant increases in frequency of sEPSCs [*Nf1*$^{+/-}$ x *Pak1*$^{-/-}$ interaction, $F_{1,62} = 4.53$, $p = 0.037$] and mEPSCs [*Nf1*$^{+/-}$ x *Pak1*$^{-/-}$ interaction, $F_{1,56} = 3.99$, $p = 0.05$,], but not amplitude of sEPSCs [no *Nf1*$^{+/-}$ x *Pak1*$^{-/-}$ interaction, $F_{1,62} = 2.68$, $p = 0.107$] and mEPSCs [n=4/4/3/3 mice/genotype and n=11/11/14/14 cells patched/genotype, no *Nf1*$^{+/-}$ x *Pak1*$^{-/-}$ interaction, $F_{1,56} = 1.03$, $p = 0.314$, Fig. 3d–f]. We detected additional significant increases of the amplitude of sEPSCs [*Pak1*$^{-/-}$ effect, $F_{1,62} = 76.63$, $p < 0.0001$] and mEPSCs [*Pak1*$^{-/-}$ effect, $F_{1,56} = 148.7$, $p < 0.0001$] in *Pak1*$^{-/-}$ and *Nf1*$^{+/-}$/*Pak1*$^{-/-}$ mice. These network changes suggest increases in presynaptic GABA release in the BLA of *Nf1*$^{+/-}$ mice, consistent with those reported in the hippocampus[16]. However, unlike the hippocampus, there appeared to be additional changes in glutamate neurotransmission in the amygdala of *Nf1*$^{+/-}$ mice.

To determine whether changes in synaptic plasticity within the amygdala might account for the social learning impairments of *Nf1*$^{+/-}$ mutants, we examined long-term potentiation (LTP) in BLA slices from these mice. Using a theta-burst stimulation (TBS) protocol[23], we elicited persistent potentiation of excitatory postsynaptic potentials (EPSPs) in *WT* mice that lasted at least beyond 60 min after stimulation. In the *Nf1*$^{+/-}$ mice, while initial potentiation was comparable to *WT* neurons, we observed significant decay over the time [n=6/6/4/4 mice/genotype and an n=7/12/8/5 cells patched/genotype; Fig. 3g–i]. By 50 min after the stimulation, the amplitude of EPSPs was no longer significantly different from those recorded 5 min prior to TBS in *Nf1*$^{+/-}$ mice [*Nf1*$^{+/-}$ effect over time $F_{14,392} = 0.6$, p = 0.838]. In contrast, LTP induced in *Nf1*$^{+/-}$/*Pak1*$^{-/-}$ mice was equivalent to that of the *WT* mice [genotype by time interaction $F_{42,392} = 3.2$, $p < 0.001$, Fig. 3g–i]. Finally, the amplitude of EPSPs, induced by TBS in *Pak1*$^{-/-}$ mice was comparable with amplitude of EPSPs recorded from BLA neurons of *WT* mice [*Pak1*$^{-/-}$ effect over time, $F_{14,392} = 2.8$, p < 0.001, Fig. 3g–i]. These results determined that *Nf1*$^{+/-}$ mice had disrupted amygdala LTP and Pak1 deletion can rescue these LTP deficits.

We next utilized mass spectrometry to measure expression levels of synaptic and neuronal proteins in the amygdala of *WT*, *Nf1*$^{+/-}$, *Nf1*$^{+/-}$/*Pak1*$^{-/-}$ and *Pak1*$^{-/-}$ mice. Our plan was to first identify proteins that were changed in *Nf1*$^{+/-}$ mice, compared to *WT*, and then determine which of those altered proteins were specifically restored in *Nf1*$^{+/-}$/*Pak1*$^{-/-}$ mice without being similarly altered by deletion of Pak1 gene alone. The group of proteins thus identified would likely be the key to the disruption of the amygdala network observed in the *Nf1*$^{+/-}$ mice. Based on our selection algorithm, out of the 380 proteins measured, we identified only three proteins in the BLA that met all three selection criteria, i.e., they were disrupted in *Nf1*$^{+/-}$ mice compared to *WT* (criteria one, 73 proteins, see Suppl. Table 1); were not changed in *Pak1*$^{-/-}$ mice compared to *WT* (criteria 2); and were rescued to near *WT* levels in *Nf1*$^{+/-}$/*Pak1*$^{-/-}$ mice (n=6/6/6/6, Table 1). There was dramatic >6 fold reductions in the levels of ADAM22 [*Nf1*$^{+/-}$ effect $F_{1,24} = 22.1$, $p < 0.001$, Fig 4a], and more modest increases in Cyclase Associated Protein (Cap1) [*Nf1*$^{+/-}$ *x Pak1*$^{-/-}$ interaction, $F_{1,23} = 7.4$, $p = 0.013$, Fig. 4a], and HSP70 [*Nf1*$^{+/-}$ *x Pak1*$^{-/-}$ interaction $F_{1,24} = 7.3$, $p = 0.014$, Fig. 4b] in the *Nf1*$^{+/-}$ mice, and all were rescued by Pak1 co-deletion. Utilizing immunocytochemistry, we further confirmed that there was a significant reduction only in the number of ADAM22 positive cells (n=5/7/6/6, *Nf1*$^{+/-}$ *effect* $F_{1,24} = 7.1$, $p = 0.015$, *Pak1*$^{-/-}$ effect $F_{1,24} = 6.7$, $p = 0.018$ Fig. 4c,f], while the numbers of CAP1 and HSP70 $t_9 = -1.0$, $p = 0.337$ and HSP70 $t_9 = -0.3$, $p = 0.748$ positive cells were unaltered [n=4/6 (one outlier removed from *WT* group), and n=4/7 respectively, Fig. 4d–e] in the BLA of *Nf1*$^{+/-}$ mice compared to *WT*. This reduction in ADAM22 positive cells was also rescued in the *Nf1*$^{+/-}$/*Pak1*$^{-/-}$ mice.

Utilizing constitutive gene deletion, one cannot definitively conclude that the social learning deficits are being rescued by selective Pak1 inhibition within the amygdala. Therefore, in a subsequent experiment we tested the effects of bilaterally injecting previously known effective doses of a Pak1 inhibitor [IPA3, or its inactive enantiomer PIR3.5 (PIR3.5) as control] into the BLA of *Nf1*$^{+/-}$ mice 30 min prior to assessment in the social familiarity test on day 1 and 2. Pre-injecting of IPA3 (100μM/100nl), and not PIR3.5, into the BLA increased preference for the novel mouse in *Nf1*$^{+/-}$ mice during the long-term social memory test. Interestingly, IPA3 injection into the BLA also increased social preference in *WT* mice during the long-term social memory test even above their baseline further supporting the role of the BLA and Pak1 activity in social learning (n=6/6/6/6, side preference x *Nf1*$^{+/-}$ interaction, $F_{1,18} = 5.2$, $p = 0.036$, and side preference x Pak1 inhibitor interaction, $F_{1,18} = 8.8$, $p = 0.008$ Fig. 5a–c). Additionally, we also confirmed that there were reduced numbers of ADAM22 immunoreactive cells in the BLA of *Nf1*$^{+/-}$ mice that was rescued in *Nf1*$^{+/-}$ mice pre-treated with the IPA3 into the BLA (n=3/3/3/3, *Nf1*$^{+/-}$ effect, $F_{1,12} = 9.7$, $p = 0.014$, and Pak1 inhibitor effect, $F_{1,12} = 10.0$, $p = 0.013$, Fig. 5d–e). To validate that the doses of IPA3 (and not the inactive enantiomer PIR3.5) blocks Pak1 function in the amygdala, we tested the effects of pre-injecting these drugs (100μM/100nl) on the increases in the number of pERK-ir cells following stimulation with DMSO, a known activator of Pak1 activity in neurons[24,25]. Injections of DMSO induced increases in pERK expression in the amygdala, whereas pre-injection with IPA3, but not PIR3.5 was able to block these effects (n=5/3/4, Suppl. Fig. 2a,d,e, $F_{2,11} = 22.6$, $p < 0.001$). Acute activation of Pak1 with injections of DMSO into the BLA of *WT* mice also caused a reduction in the

number of ADAM22-ir cells and IPA3 (and not PIR3.5) pre-injections blocked those reductions as well (n=5/3/4, $F_{2,11} = 6.2$, $p = 0.020$; Suppl. Fig. 2b,d,e).

Discussion

In summary, our findings demonstrated that *Nf1*$^{+/-}$ mice exhibit a selective deficit in social learning and the mechanisms underlying these social learning deficits appear to be disruption in the regulation of classical MAPK pathway in the amygdala. We have also determined that *Nf1*$^{+/-}$ mice show disruptions of synaptic plasticity (LTP), GABA-mediated inhibition and glutamate excitation of neurons, and altered expression of important synaptic proteins ADAM22 and HSP70 within the amygdala. ADAM22 is a synaptic protein that is thought to be critical for regulating the strength of glutamate neurotransmission and LTP, and shown to specifically anchor AMPA receptors on the post-synaptic terminals in the hippocampus[26–28]. Therefore, although the role of ADAM22 in anchoring AMPA receptors specifically in the amygdala has not yet been directly demonstrated, significant decreases in ADAM22 in *Nf1*$^{+/-}$ mice in the amygdala could be predicted to cause similar failure to anchor AMPA receptors to the post-synaptic membrane and sustain LTP as demonstrated in *Nf1*$^{+/-}$mice (see Suppl. Fig. 1b for hypothetical illustration), Similarly, HSP70 is thought to be critical for anchoring the GABA synthetic mechanisms to the presynaptic terminals[29] and increases in the expression levels of HSP70 could lead to increases specifically in pre-synaptic GABA release and increased frequency of sIPSCs as demonstrated in this study. These increases in GABA release may also compensate for some of the glutamate neurotransmission disequilibrium and could be a potential explanation for *Nf1*$^{+/-}$ mice not developing severe seizures that are seen in *ADAM22*$^{-/-}$ mice[30]. CAP1 is a protein that plays an important role in the regulation of actin polymerization and synaptic remodeling, processes that are critical for long-term memory[31].

The social deficits and all of the aforementioned amygdala disruptions in *Nf1*$^{+/-}$ mice were rescued by co-deletion of *Pak1* gene. Pharmacological blockade of Pak1 function directly within the amygdala also rescued the social deficits seen in *Nf1*$^{+/-}$ mice. These results suggest that Pak1 inhibition, consistent with the recently reported neurofibroma tumor reductions in these children[32], may represent a therapeutic target of interest for the treatment of NF1-related social and learning symptoms that pose a significant burden to these children[1,32]. Co-deletion of Pak1 gene, which rescued the behavioral deficits seen in *Nf1*$^{+/-}$ mice, also restored the changes in the synaptic protein expressions, and as predicted by our hypotheses, rescued the network disruptions in the amygdala, and normalized amygdala LTP. The precise mechanisms involved in these gene expression changes induced by *Nf1* haplo-insufficiency and their rescue by Pak1 deletion are yet to be determined. However, there is supportive evidence that inhibiting Pak1 levels will reduce CAP1 levels in the CNS[33], and the genes for Pak1, Erk1 and LGl-4 (the endogenous CNS ligand for ADAM22) are all located on murine chromosome 7. Moreover, it has been shown, that single injection of Pak1 inhibitor completely rescues seizures and behavioral abnormalities such as hyperactivity and repetitive movements in Fragile X mental retardation 1 (*Fmr1*$^{-/-}$) mice[34]. Finally, due to the increases in co-occurrence of NF1 and ASD[35,36], these findings may also have important implications for the molecular targets for the remediation of social deficits in some forms of ASD. Indeed, a recent deep brain stimulation report show that directly

stimulating the BLA region in a severely autistic child was effective in improving core symptoms of the ASD in the emotional, social, and even cognitive domains over a follow up of 24 months[37]. To conclude, we have demonstrated selective deficits in social learning and underlying disruptions in the amygdala network caused by a single (*Nf1)* gene mutation. We have also provided a potential novel therapeutic approach towards ameliorating these disabling behavioral symptoms seen in patients with NF1 and some forms of ASD.

Online Methods

Animals

Most experiments were conducted using adult male mice, except for cellular assay and western blotting experiment, which was done in mice 2–3 days postnatal and electrophysiology experiments were done in 2–3 month old mice. The mouse strains tested were bred on a C57BL/6J background and included: (1) *WT*, (2) $Nf1^{+/-}$, (3) $Nf1^{+/-}/Pak1^{-/-}$ and (4) $Pak1^{-/-}$ mice. The $Nf1^{+/-}$ mice were obtained from Tyler Jacks at the Massachusetts Institute of Technology (Cambridge, MA), and $Pak1^{-/-}$ mice were obtained from Jonathan Chernoff (Fox Chase Cancer Center). To generate the $Nf1^{+/-}/Pak1^{-/-}$ *mice*, $Pak1^{-/-}$ mice were intercrossed with the $Nf1^{+/-}$ strain. All mice were singly housed, given food and water ad libitum and maintained on a 12 hour light-dark cycle (7:00 am/7:00 pm) at 72°F. Animal care procedures were conducted in accordance with the NIH Guidelines for the Care and Use of Laboratory Animals (NIH Publication no. 80-23) revised 1996. All procedures have been approved by the Indiana University School of Medicine Institutional Animal Care and Use Committee (protocol no. 10326).

Behavioral testing

Behavioral testing reported in Figure 1a–d, g–h, I, and j were done in the same cohort of mice which were tested in the social behavior test on day 1, elevated plus maze (Fig. 1g) on day 2, olfactory test on day 3, and behavioral despair on day 4. Behavioral testing reported in Figure 1e and f were in done in the same cohort of mice, which were tested in the novel object recognition test on day 1, and passive avoidance test on day 2. Behavioral testing reported in Figure 2b–e, f, g, and h were done in the same cohort of mice which were tested in the social behavior test on day 1, elevated plus maze (Fig. 1g) on day 2, olfactory test on day 3, and behavioral despair on day 4. Social behavior tests reported in Figure 4 were done in a separate cohort of mice in a crossover design with 5 days between cross over. All behavioral tests were videotaped and independently scored at a later time by two individuals who were unaware of the animals' genotype. Following each test, the apparatus were cleaned with 90% ethanol and dried.

Social behavior tests

The social interaction test was conducted as previously described[39,40]. Four 10 minutes sessions were conducted including (1) Day 1: acclimation (two empty cylindrical cages); (2) Day 1: 5 min after acclimation, preference for social interaction [novel mouse (mouse 1) and an empty cage]; (3) Day 1: 5 min after initial exposure to the mouse 1, a short-term social learning was done with mouse 1 (the now familiar mouse) and mouse 2 (a novel mouse); and (4) long-term social learning 24 hrs later [familiar mouse (mouse 2) and a novel mouse

(mouse 3)]. Following the “short-term social learning” session, the “novel” mouse was removed from the apparatus, and the “test” mouse was allowed to interact with the “familiar” mouse for an additional 45 minutes. The “stimulus” mice used for the social behavior tests were age-matched, adult male C57BL/6J mice that had no previous contact with the “test” mice.

Novel Object Recognition Test

The novel object recognition test (NORT) was used to measure short-term memory retention. The apparatus consisted of an opaque plexiglass chamber of (50 × 50 × 50 cm height). Two objects presenting similar textures, colors and sizes (2 cylinder) were placed in opposite corners of the chamber. Between trials, the objects and the box are cleaned with 70% ethanol. The habituation session consisted of placing a mouse in the chamber for 10 min, and at the end of each session the mouse was returned to the homecage. Two hours later, the mouse was placed in the chamber with a similar cylinder in each corner, and the time exploring (nose within 1 inch from object) the two objects was assessed for 10 min. 30 min later, the mouse was placed in the chamber with the now familiar cylinder and an unfamiliar cube in each corner. The time exploring (nose within 1 inch from object) the two dissimilar objects was assessed for 10 min.

Passive Avoidance Memory Test

This passive avoidance task is a one trial fear-motivated avoidance task in which the mouse learns to refrain from stepping from a lighted chamber through a door to an apparently safer enclosed dark chamber where the mouse previously received a shock. The training chambers consist of one compartment (20×40×30cm height) that is lighted by an overhead stimulus light (40W bulb) and the other compartment (20×20×30cm height), which is black and enclosed so as to remain dark. An automatic guillotine door separated the two compartments.

On habituation day the mouse is placed in a lighted compartment facing away from the dark compartment; allowed to explore for 30 sec; then the door to the dark chamber is raised. When the mouse enters the dark compartment, the guillotine door is closed. 5 min later the mouse removed and returned to the home cage. On the training day, the test is repeated, except that upon entering the dark chamber the door is closed and the mouse receives a footshock (0.5 mA, 2 sec duration) through a grid. 30 seconds after the footshock the mouse is returned to the homecage. On testing day, the test is repeated and the latency to enter the dark chamber with front 2 paws is determined.

Elevated plus maze

The elevated plus-maze (EPM) was conducted as previously described[41] where mice were allowed to freely explore the entire apparatus for five minutes. This procedure was again performed 24 hours later as a measure of avoidance learning. An arm entry was defined as having all four paws into the arm of the EPM.

The Porsolt forced swim test

The forced swim test was utilized to measure aspects of behavioral despair[41,42]. The forced swim apparatus consisted of a cylindrical chamber constructed of clear Plexiglas with a diameter of 8.5 inches and height of 10 inches. For each trial, the chamber was filled with 25 ± 1°C water. The "test" mouse was then gently placed into the cylinder for 15 min. Twenty-four hours later the mice were re-exposed to the same conditions for an additional six minutes trial. Immobility was considered the cessation of limb movements except minor involuntary hind limb movements.

Olfactory habituation test

The mice were placed in a clean cage, and were assessed for time spent sniffing cotton tipped swabs suspended from the cage lid. The cotton swabs were dipped in (1) water, (2) almond extract (1:100 dilution) or (3) wiped in a zig-zag pattern across the bottom surface of a cage that contained an unfamiliar mouse (a singly housed male mouse (C57BL/6J). Sequences of three identical swabs were assayed for each odor as follows: water, water, water, almond, almond, almond, unfamiliar cage, unfamiliar cage, unfamiliar cage. Each swab was presented for 2 min for a total session lasting 18 min per mouse.

Isolation and culture of neuronal cells from murine strains

Neurons were obtained from the frontal cortical and amygdala regions mice 2–3 days postnatal that were aseptically dissected and cultured from each respective genotype (*WT*, $Nf1^{+/-}$, $Nf1^{+/-}/Pak1^{-/-}$, $Pak1^{-/-}$). Following dissection of each respective brain region, neuronal cells were isolated by dissociation both enzymatically and mechanically (via trituration through a flame-polished Pasteur pipette) in a Papain solution (12 units/ml; Worthington) as described previously[41]. For this experiment, the neuronal cultures were assigned to one of two experimental conditions: (i) at basal levels and (ii) following the application of recombinant murine stem cell factor (SCF; PreproTech) at 10 ng/ml. SCF was applied to the neuronal cultures for 2 min. The cells were then washed with ice-cold PBS and lysed in buffer, as described below.

Immunoblotting ERK/pERK in mouse cortical and amygdala neurons

Whole cell protein extracts were obtained from the frontal cortical and amygdala regions of mice 2–3 days postnatal and placed in lysis buffer (50mM Tris pH 7.4, 150mM NaCl, 2mM EDTA pH 8.0, 1% Triton X-100, 1mM PMSF, 1mM NaF, 1mM Na3VO4, 10% glycerol and protease inhibitors). The samples were sonicated and cellular debris was removed by centrifugation at 13,000g for 30 min at 4°C. Protein concentrations were determined using a BCA assay (Thermo Scientific). Equivalent amounts of protein was electrophoresed on 10% SDS-PAGE gels, transferred to PVDF membranes (GE Healthcare, Little Chalfont, UK), and detected by Western blotting using the ECL Plus system (Amersham Biosciences). Antibodies used were phospho-ERK1/2 Antibody (cat. no. 4370, Cell Signaling Technology), ERK1/2 antibody (cat. no. 4695, Cell Signaling Technology), and GAPDH (cat. no. MAB374, Millipore). Cell Signaling reports the following: the ERK1/2 monoclonal antibody p44/42 MAP Kinase (137F5) Rabbit mAb detects endogenous levels of total p44/42 MAP kinase (Erk1/Erk2) protein. The antibody does not cross-react with JNK/SAPK

or p38 MAP kinase; and the ERK1/2 anti-phospho ERK monoclonal antibody is produced by immunizing rabbits with a synthetic phosphopeptide corresponding to residues surrounding Thr202/Tyr204 of human p44 MAP kinase, and binds to endogenous levels of p44 and p42 MAP Kinase (Erk1 and Erk2) when dually phosphorylated at Thr202 and Tyr204 of Erk1 (Thr185 and Tyr187 of Erk2), and singly phosphorylated at Thr202. This antibody does not cross-react with the corresponding phosphorylated residues of either JNK/SAPK or p38 MAP kinases. All mice were delivered to RK, whom was unaware of the animals' genotype.

Immunostaining of pERK cells in amygdala of mice exposed to novel mouse

Wildtype and *Nf1*$^{+/-}$ mice were habituated to the social learning apparatus with two empty cages, and then 24 hrs later placed in social learning apparatus with a novel mouse in one cage. Mice were then placed in homecage for 80 min then anesthetized with Isoflurane and perfused transcardially with 250 ml 0.1M PBS, followed by 250 ml of 0.1M PB containing 4% paraformaldehyde and 3% sucrose and processed for immunohistochemistry, and to yield 4 alternative sets of serial coronal sections (30 μm). A standard immunohistochemical procedure was then performed as described in detail previously[43], utilizing a monoclonal rabbit anti-phospho-ERK1/2 antibody (1:200 dilution; cat. no. 4370, Cell Signaling).

Protein expression analysis

Tissue slices were homogenized in 50 mM ammonium bicarbonate, and whole cell protein extracts were obtained from brain slices in lysis buffer (30mM Tris, pH 7.4, 150mM NaCl, 1% Triton X-100, 0.1% SDS, 1mM PMSF, 10mM EDTA, 1mM Na2CO3, 160mM NaF, complete protease inhibitor) with ProteoSpin total protein detergent clean up micro kit (Norgen, Canada). BCA Protein Assay Kit (Pierce, Rockford, IL) was utilized to determine protein concentrations of the lysates (Pierce, Rockford, IL). Protein samples were reduced through DTT and alkylation was achieved by adding IAA. The protein samples then subjected to tryptic digestion at 37°C overnight and quenched through the addition of neat formic acid. LC-MS/MS analyses of the tryptic digests were performed using a Dionex 3000 Ultimate nano-LC system (Dionex, Sunnyvale, CA) interfaced to LTQ Orbitrap hybrid mass spectrometer (Thermo Scientific, San Jose, CA). Prior to separation, a 2-μl aliquot of trypsin digestion (1.5 μg protein equivalent) was loaded on PepMap300 C18 cartridge (5 μm, 300 Å, Dionex) and eluted through the analytical column (150 mm × 100 μm i.d, 200 Å pores) packed with C18 magic (Michrom Bioresources, Auburn, CA). Peptides originating from protein tryptic digests were separated using a reversed-phase gradient from 3–55% B, 99.9% acetonitrile with 0.1% formic at 500 nl/min flow rate and passed through an ADVANCE ionization source (Michrom Bioresources, Auburn, CA). Switching between MS scan and CID-MS, eluted LC products undergo an initial full-spectrum MS scan from m/z 300 to 2000 in the Orbitrap at 15,000 mass resolutions. Subsequently CID-MS (at 35% normalized collision energy) was performed. The total cycle (6 scans) is continuously repeated for the entire LC-MS run under data-dependent conditions. Mascot version 2.1.3 was used for all search results against Swiss-Prot database for house mouse, and the quantitative analysis of proteins was carried out using ProteinQuant Suit developed at Indiana University. The combined master files were then incorporated with their corresponding mzXML files and were submitted to ProteinQuant as described previously[44]. Pathway analyses were then

conducted on proteins that showed significant differences between WT and Nf1+/−, and were restored in the Nf1+/−/Pak1−/− genotype utilizing INGENUITY systems software (Redwood City, CA). Protein expression data were further analyzed using one-way and two-way analyses of variance. All mouse tissue was given to the proteomics core collaborators, whom were unaware of the animals' genotype.

Electrophysiology

The electrophysiological recordings were performed in 2–3 month old mice as described previously[45]. Briefly, following decapitation, the brains were rapidly removed and placed in oxygenated artificial cerebrospinal fluid (ACSF) [130mM NaCl; 3.5mM KCl; 1.1mM KH2PO4; 1.3mM MgCl2; 2.5mM CaCl2; 30mM NaHCO3; 10mM glucose], and coronal slices (350 μM) were prepared containing the basolateral amygdala (BLA). After initial at least 30 min incubation at 30°C in oxygenated ACSF slices were transferred to a recording chamber mounted on the stage of a Nikon E600FN Eclipse (Nikon Instruments, Melville, NY) microscope and perfused with ACSF [2–3 ml per minute] heated to 30°C. Whole-cell patch-clamp recordings were obtained using standard techniques. Borosilicate glass electrodes (WPI, Sarasota, FL) (resistance 3–6 MΩ) were prepared with a potassium gluconate based recording solution [130mM K-Gluconate, 3mM KCl, 3mM MgCl2, 5mM phosphocreatine, 2mM K-ATP, 0.2mM NaGTP, 10mM HEPES] and were maintained at a holding potential of −60 mV. BLA pyramidal neurons were identified according to their characteristic size and shape[46]. At the start of each experiment, except LTP experiments, a series of current clamp protocols were performed to further validate the identity of BLA projection neurons. Drugs were added directly into the ACSF at the required concentration. The spontaneous inhibitory postsynaptic currents (sIPSCs) and miniature IPSCs (mIPSC) [in the presence of 1 μM tetrodotoxin (TTX)] were recorded at a holding potential of −55 mV in the presence of DNQX (20 μM), CPP (10 μM). The spontaneous excitatory postsynaptic currents (sEPSCs) and miniature EPSCs (mEPSCs) [in 1 μM TTX] were acquired at a holding potential of −60 mV in the presence of $GABA_A$ antagonist bicuculline methochloride (10 μM) and $GABA_B$ antagonist CGP52432 (1 μM). The spontaneous and miniature currents were captured continuously for 1 min and detected and analyzed afterwards using the MiniAnalysis (Synaptosoft, Decatur, GA).

Excitatory postsynaptic potentials (EPSPs) onto BLA projection neurons were evoked in current clamp as previously described[47]. The $GABA_B$ antagonist CGP52432 (1 μM) was added to ACSF and $GABA_A$ antagonist picrotoxin (50 μM) was included into the recording solution. The holding potential was adjusted to −70 mV, except during theta-burst stimulation (TBS) when the potential was adjusted to −55 mV to facilitate spike firing. A 10 min baseline period was recorded in each experiment and recordings continued for at least 60 min after LTP induction. The TBS consisted of 40 msec duration, 100 bursts delivered at 5 Hz for 5 sec (100 pulses total). Evoked postsynaptic potentials were analyzed using the pClamp 10.3 (Molecular Devices, Sunnyvale, CA). All chemicals, except CPP and CGP52432 (Tocris Biosciences, Ellisville, MO), were purchased from Sigma-Aldrich (St. Louis, MO). All mice were brought to AIM, who was unaware of the animals' genotype.

Immunohistochemistry for (ADAM22, CAP1 and HSP70) in the Basolateral Amygdala

Mice were anesthetized with Halothane then perfused transcardially with 250 ml 0.1M PBS, followed by 250 ml of 0.1 M PB containing 4% paraformaldehyde and 3% sucrose and processed for immunohistochemistry as described previously. A standard immunohistochemical procedure was then performed as described in detail previously[43] utilizing the following antibodies on separate serial sections: affinity purified rabbit anti-ADAM22 polyclonal antibody (1:200 dilution; cat. no. ab56122, Abcam, Cambridge, MA); rabbit anti-CAP1 polyclonal antibody (1:200 dilution, cat. no. sc134637, Santa Cruz Biotechnology, Santa Cruz CA); affinity purified rabbit anti-HSP70 affinity purified polyclonal antibody (1:100 dilution, cat. no. NBP1-00880, Novus Biologicals, Littleton Co). Abcam reports the following: The ADAM22 immunogen was a synthetic peptide based on the metalloproteinase domain of human ADAM22, and the ADAM22 antibody is reactive with mouse ADAM22 protein at the predicted band in Western Blots. Santa Cruz reports that the CAP1 rabbit polyclonal antibody was raised against amino acids 14–74 mapping near the N-terminus of CAP1 of human origin and is reactive with mouse CAP1 protein at the predicted band in Western Blots. Novus Biologicals reports that the CAP1 antibody was raised against the synthetic peptide corresponding to the residues surrounding Phenylalanine 245 of human HSP70, and reactive with mouse HSP70 protein at the predicted band in Western Blots.

Photography and cell counts

Photomicrographs were obtained using a Leica brightfield microscope using N plan 5x, 10x, 20x and 40x objective lenses (model DMLB, Leica Microsystems), a SPOT digital camera (RT color, Diagnostics Instruments Inc., Sterling Heights, MI) and SPOT 4.7.1.32 for Windows digital imaging software. Photographic plates were prepared in CorelDraw X5 for Windows (Eden Prairie, MN). Immunoreactive (ir) cells in the BLA were counted on a 400 x magnification photomicrograph and then verified at 400X using a Leica DMLB binocular microscope (Leica Microsystems) by an investigator (PLJ), who was blind to the experimental treatment of each animal.

Site Directed Injections of a Pak1 Inhibitor into the BLA of NF1 mice

Stereotaxic Cannula Placement—Prior to and during surgery, mice were anesthetized with a nose cone connected to an isoflurane system (MGX Research Machine; Vetamic) and placed in an ultraprecise stereotaxic apparatus for rodents (900 series Ultraprecise Kopf Instruments). Bilateral injection cannulae (26 gauge; Plastics One) were implanted into the BLA (AP: −1.5; ML: +/− 3.35; DV: −4.55; and incisor bar was set at −3.0 mm to keep lambda and bregma suture at same DV) according to a standard stereotaxic atlas of the mouse brain[48]. The cannulas were secured to the skull with three stainless steel screws (2.8 mm, Plastic One, Roanoke VA) and Loctite adhesive. Upon completion of surgery a dummy cannula that went the length of the guide were screwed in place. All mice then received buprenex 1 mg/kg s.c. and were placed on a warming pad until fully recovered.

Intracranial Injection Procedures—At 30 min prior to the novel mouse exposure and the long term social memory testing the next day, *WT* and *Nf1*$^{+/-}$ mice received

microinjections via an injector (33 gauge, Plastic Products) that fit into, and extended 0.5 mm beyond, the guide cannula. A 10 µl Hamilton syringe was placed on an infusion pump (Harvard Apparatus, Holliston, MA, model PHD 2000) and connected to the injection cannula via polyethylene (PE 50) tubing. The pump delivered 100 nl of either the Pak1 inhibitor IPA3 (cat. no. 3622, Tocris Biosciences, n=6) or the inactive enantiomer PIR3.5 (cat no. 4212, Tocris Biosciences, n=6) dissolved in DMSO into the BLA per site over 30 seconds. The injection cannula remained in place for an additional minute to ensure complete delivery of the solution and proper flow was confirmed in the cannulae after removal. All injection sites were verified using 400X magnification Leica DMLB brightfield microscope.

Statistical Analyses of Data

For behavior tests in figure 1 with western blotting and immunohistochemistry with *WT* and $Nf1^{+/-}$ mice data were analyzed using one-way or analyses of variance (ANOVAs) with genotype as the main factor and when applicable a side preference or time as a repeated measure. For behavior tests in figure 2 with $Nf1^{+/-}$, $Nf1^{+/-}/Pak1^{-/-}$ and $Pak1^{-/-}$ mice, data were analyzed using one-way or analyses of variance (ANOVAs) with genotype as the main factor and when applicable a side preference or time as a repeated measure. For electrophysiology in figure 3, and proteomics and immunohistochemistry in Table 1 and Figure 4 and behavior tests in figure 5 with *WT*, $Nf1^{+/-}$, $Nf1^{+/-}/Pak1^{-/-}$ and $Pak1^{-/-}$ mice, data were analyzed using a two-way analyses of variance (ANOVAs) with $Nf1^{+/-}$ and $Pak1^{-/-}$ as the main factors or genotype and drug treatment as main factors and when applicable a side preference or time as a repeated measure. Significant effects were further analyzed using post hoc Fisher's protected least significant difference (FLSD) tests for between subjects effects of multiple groups, or a 2 way paired or independent t-test (as appropriate) for 2 group comparisons. A Dunnett's post-hoc test was used to compare within subject over time effects in Fig. 3. A Levene's Test was conducted prior to analyses to assess for equality of variance. To protect against type I errors, the n's per group were considered acceptable if significant ($P < 0.05$) in the previously mentioned analyses. In cases where there was a trend towards significance ($P > 0.05$ –0.060), power analyses were done to determine if the n's per group were sufficiently powered, and to protect against type II errors. An outlier was detected for one animal in the behavioral assessments in Figure. 1c and also in Figure 5a with a Grubb's test, and were therefore excluded. There were no missing data for cell assays, westerns, proteomics, or electrophysiology. For proteomics analyses, using Pathway analyses in INGENUITY software, there were no missing data points. However in a subsequent secondary analyses using one-way ANOVAs, there was one missing data point in the CAP1 *WT* group due to an outlier that was >2 standard deviations from the mean (Fig. 4a). For immunohistochemistry, one data point was missing in the CAP1 *WT* group (Fig. 4d), and the HSP70 $Nf1^{+/-}$ group (Fig. 4e) due to there being no representative coronal slice containing the amygdala at that level of bregma, and another data point in the CAP1 WT group that was an outlier.

Supplementary Material

Refer to Web version on PubMed Central for supplementary material.

Acknowledgments

Supported by grants from NCATS, NIH UL1RR025761/TR000006, R01 MH52619 and MH065702 (to AS), predoctoral fellowship to JPS (TL1 RR 025759), and R01 CA74177-06 (to DWC).

Reference List

1. Johnson NS, Saal HM, Lovell AM, Schorry EK. Social and emotional problems in children with neurofibromatosis type 1: evidence and proposed interventions. J Pediatr. 1999; 134:767–772. [PubMed: 10356149]
2. Barton B, North K. Social skills of children with neurofibromatosis type 1. Dev Med Child Neurol. 2004; 46:553–563. [PubMed: 15287247]
3. Noll RB, et al. Social, emotional, and behavioral functioning of children with NF1. American journal of medical genetics Part A. 2007; 143A:2261–2273. [PubMed: 17726688]
4. Lehtonen A, Howie E, Trump D, Huson SM. Behaviour in children with neurofibromatosis type 1: cognition, executive function, attention, emotion, and social competence. Dev Med Child Neurol. 2013; 55:111–125. [PubMed: 22934576]
5. Huijbregts SC, de Sonneville LM. Does cognitive impairment explain behavioral and social problems of children with neurofibromatosis type 1? Behavior genetics. 2011; 41:430–436. [PubMed: 21184163]
6. Huijbregts S, Jahja R, De Sonneville L, de Breij S, Swaab-Barneveld H. Social information processing in children and adolescents with neurofibromatosis type 1. Dev Med Child Neurol. 2010; 52:620–625. [PubMed: 20187875]
7. Garg S, et al. Neurofibromatosis Type 1 and Autism Spectrum Disorder. Pediatrics. 201310.1542/peds.2013-1868
8. Garg S, et al. Autism and other psychiatric comorbidity in neurofibromatosis type 1: evidence from a population-based study. Dev Med Child Neurol. 2013; 55:139–145. [PubMed: 23163236]
9. Walsh KS, et al. Symptomatology of autism spectrum disorder in a population with neurofibromatosis type 1. Dev Med Child Neurol. 2013; 55:131–138. [PubMed: 23163951]
10. Pride NA, et al. The genetic and neuroanatomical basis of social dysfunction: Lessons from neurofibromatosis type 1. Hum Brain Mapp. 201310.1002/hbm.22334
11. Truitt WA, et al. From anxiety to autism: spectrum of abnormal social behaviors modeled by progressive disruption of inhibitory neuronal function in the basolateral amygdala in Wistar rats. Psychopharmacology. 2007; 191:107–118. [PubMed: 17277936]
12. Maaswinkel H, Baars AM, Gispen WH, Spruijt BM. Roles of the basolateral amygdala and hippocampus in social recognition in rats. Physiol Behav. 1996; 60:55–63. [PubMed: 8804643]
13. Todd RM, Anderson AK. Six degrees of separation: the amygdala regulates social behavior and perception. Nature neuroscience. 2009; 12:1217–1218. [PubMed: 19783979]
14. Zhu Y, Ghosh P, Charnay P, Burns DK, Parada LF. Neurofibromas in NF1: Schwann cell origin and role of tumor environment. Science. 2002; 296:920–922. [PubMed: 11988578]
15. Costa RM, et al. Mechanism for the learning deficits in a mouse model of neurofibromatosis type 1. Nature. 2002; 415:526–530. [PubMed: 11793011]
16. Cui Y, et al. Neurofibromin regulation of ERK signaling modulates GABA release and learning. Cell. 2008; 135:549–560. [PubMed: 18984165]
17. Sankoorikal GM, Kaercher KA, Boon CJ, Lee JK, Brodkin ES. A mouse model system for genetic analysis of sociability: C57BL/6J versus BALB/cJ inbred mouse strains. Biological psychiatry. 2006; 59:415–423. [PubMed: 16199013]
18. Crawley JN, et al. Social approach behaviors in oxytocin knockout mice: comparison of two independent lines tested in different laboratory environments. Neuropeptides. 2007; 41:145–163. [PubMed: 17420046]
19. Brittain JM, et al. Suppression of inflammatory and neuropathic pain by uncoupling CRMP-2 from the presynaptic Ca(2)(+) channel complex. Nature medicine. 2011; 17:822–829.

20. Le LQ, Parada LF. Tumor microenvironment and neurofibromatosis type I: connecting the GAPs. Oncogene. 2007; 26:4609–4616. [PubMed: 17297459]
21. Wang Y, et al. ERK inhibition rescues defects in fate specification of Nf1-deficient neural progenitors and brain abnormalities. Cell. 2012; 150:816–830. [PubMed: 22901811]
22. Zhang YY, et al. Nf1 regulates hematopoietic progenitor cell growth and ras signaling in response to multiple cytokines. J Exp Med. 1998; 187:1893–1902. [PubMed: 9607929]
23. Li C, Dabrowska J, Hazra R, Rainnie DG. Synergistic activation of dopamine D1 and TrkB receptors mediate gain control of synaptic plasticity in the basolateral amygdala. PloS one. 2011; 6:e26065. [PubMed: 22022509]
24. Deacon SW, et al. An isoform-selective, small-molecule inhibitor targets the autoregulatory mechanism of p21-activated kinase. Chem Biol. 2008; 15:322–331. [PubMed: 18420139]
25. Kalwat MA, Yoder SM, Wang Z, Thurmond DC. A p21-activated kinase (PAK1) signaling cascade coordinately regulates F-actin remodeling and insulin granule exocytosis in pancreatic β cells. Biochem Pharmacol. 2013; 85:808–816. [PubMed: 23246867]
26. Fukata Y, et al. Epilepsy-related ligand/receptor complex LGI1 and ADAM22 regulate synaptic transmission. Science. 2006; 313:1792–1795. [PubMed: 16990550]
27. Ohkawa T, et al. Autoantibodies to epilepsy-related LGI1 in limbic encephalitis neutralize LGI1-ADAM22 interaction and reduce synaptic AMPA receptors. J Neurosci. 2013; 33:18161–18174. [PubMed: 24227725]
28. Fukata Y, et al. Disruption of LGI1-linked synaptic complex causes abnormal synaptic transmission and epilepsy. Proc Natl Acad Sci USA. 2010; 107:3799–3804. [PubMed: 20133599]
29. Hsu CC, et al. Association of L-glutamic acid decarboxylase to the 70-kDa heat shock protein as a potential anchoring mechanism to synaptic vesicles. J Biol Chem. 2000; 275:20822–20828. [PubMed: 10781586]
30. Sagane K, et al. Ataxia and peripheral nerve hypomyelination in ADAM22-deficient mice. BMC Neurosci. 2005; 6:33. [PubMed: 15876356]
31. Hubberstey AV, Mottillo EP. Cyclase-associated proteins: CAPacity for linking signal transduction and actin polymerization. FASEB journal : official publication of the Federation of American Societies for Experimental Biology. 2002; 16:487–499. [PubMed: 11919151]
32. Yang FC, et al. Nf1-dependent tumors require a microenvironment containing Nf1+/−- and c-kit-dependent bone marrow. Cell. 2008; 135:437–448. [PubMed: 18984156]
33. Nakatani N, et al. Expression analysis of actin-related genes as an underlying mechanism for mood disorders. Biochem Biophys Res Commun. 2007; 352:780–786. [PubMed: 17141188]
34. Dolan BM, et al. Rescue of fragile X syndrome phenotypes in Fmr1 KO mice by the small-molecule PAK inhibitor FRAX486. Proc Natl Acad Sci USA. 2013; 110:5671–5676. [PubMed: 23509247]
35. Martin I, et al. Transmission disequilibrium study of an oligodendrocyte and myelin glycoprotein gene allele in 431 families with an autistic proband. Neuroscience research. 2007; 59:426–430. [PubMed: 17897745]
36. Marui T, et al. Association between the neurofibromatosis-1 (NF1) locus and autism in the Japanese population. American journal of medical genetics Part B, Neuropsychiatric genetics : the official publication of the International Society of Psychiatric Genetics. 2004; 131B:43–47.
37. Sturm V, et al. DBS in the basolateral amygdala improves symptoms of autism and related self-injurious behavior: a case report and hypothesis on the pathogenesis of the disorder. Front Hum Neurosci. 2012; 6:341. [PubMed: 23346052]
38. Paxinos, G.; Franklin, KBJ. The Mouse Brain in Stereotaxic Coordinates. Academic Press; 2008.
39. Sankoorikal GM, Kaercher KA, Boon CJ, Lee JK, Brodkin ES. A mouse model system for genetic analysis of sociability: C57BL/6J versus BALB/cJ inbred mouse strains. Biological psychiatry. 2006; 59:415–423. [PubMed: 16199013]
40. Crawley JN, et al. Social approach behaviors in oxytocin knockout mice: comparison of two independent lines tested in different laboratory environments. Neuropeptides. 2007; 41:145–163. [PubMed: 17420046]
41. Brittain JM, et al. Suppression of inflammatory and neuropathic pain by uncoupling CRMP-2 from the presynaptic Ca(2)(+) channel complex. Nature medicine. 2011; 17:822–829.

42. Porsolt RD, Le Pichon M, Jalfre M. Depression: a new animal model sensitive to antidepressant treatments. Nature. 1977; 266:730–732. [PubMed: 559941]

43. Johnson PL, Truitt WA, Fitz SD, Lowry CA, Shekhar A. Neural pathways underlying lactate-induced panic. Neuropsychopharmacology. 2008; 33:2093–2107. [PubMed: 18059441]

44. Mann B, et al. ProteinQuant Suite: a bundle of automated software tools for label-free quantitative proteomics. Rapid communications in mass spectrometry: RCM. 2008; 22:3823–3834. [PubMed: 18985620]

45. Molosh AI, et al. NPY Y(1) Receptors Differentially Modulate GABA(A) and NMDA Receptors via Divergent Signal Transduction Pathways to Reduce Excitability of Amygdala Neurons. Neuropsychopharmacology. 201310.1038/npp.2013.33

46. McDonald AJ, Mascagni F, Mania I, Rainnie DG. Evidence for a perisomatic innervation of parvalbumin-containing interneurons by individual pyramidal cells in the basolateral amygdala. Brain research. 2005; 1035:32–40. [PubMed: 15713274]

47. Li C, Dabrowska J, Hazra R, Rainnie DG. Synergistic activation of dopamine D1 and TrkB receptors mediate gain control of synaptic plasticity in the basolateral amygdala. PloS one. 2011; 6:e26065. [PubMed: 22022509]

48. Paxinos, G.; Franklin, KBJ. The Mouse Brain in Stereotaxic Coordinates. Academic Press; 2008.

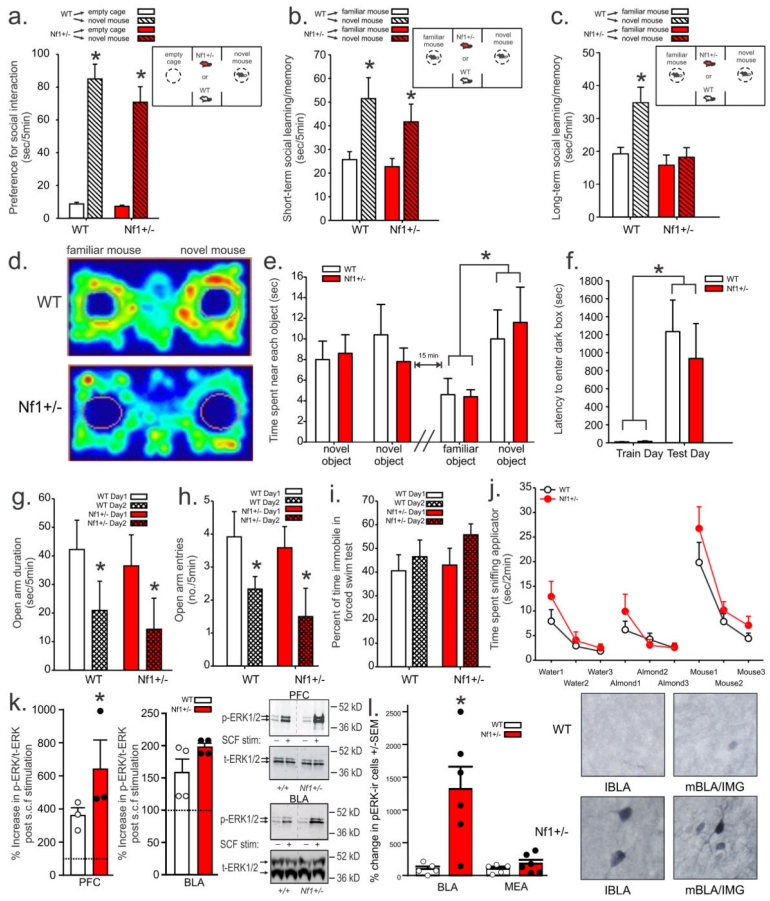

Figure 1. *Nf1*$^{+/-}$ mice show selective deficits in long-term social learning and increased MAPK activation in the amygdala compared to wild-type (*WT*) mice

Figure 1a–c depicts the time spent sniffing wire cages containing "stimulus" mice in a three-chambered apparatus (refer to insets that illustrate the orientation of cages and when cages were empty or contained a novel or familiar mouse). No differences were detected between strains in (**a**) preference for social interaction or (**b**) short-term social learning (1–3 min. following exposure to "test" mouse). **c–d**) Unlike *WT*, *Nf1*$^{+/-}$ mice show deficits in long-term social learning, as measured by preference for social novelty (24 hrs. following exposure to "test" mouse). **(d)** represents comprehensive heat maps of time spent in each region. No differences were observed in learning in the (**e**) novel object recognition test or (**f**) passive avoidance test; anxiety states in the (**g–h**) elevated plus maze; depression/despair in the (**i**) forced swim test; or olfaction in an (**j**) olfactory habituation. **(k)** The *Nf1*$^{+/-}$ genotype is associated with MAPK hyperexcitation in neuronal cultures from the prefrontal cortex (PFC, left graph. Western blotting was used to quantify pERK1/2 in cultured cortical neurons at basal levels and 2 min following stimulation with SCF (10 ng/ml), and total Erk1/2 was used as loading controls. Compared to *WT* mice, MAPK hyperexcitation was not apparent in the basolateral amydala (BLA) region of *Nf1*$^{+/-}$ mice in (k, right graph and cropped western blots; full-length blots/gels are presented in Suppl. Fig. 3), but it **(l)** was apparent in cells immunoreactive for pERK within the BLA, but not medial amygdala (MEA) of *Nf1*$^{+/-}$ mice exposed to a novel mouse. Graphs depict mean ± SEM for *WT*

(white) and *Nf1*$^{+/-}$ (red) mice. *$P < 0.05$. High magnification photographs (I, right) show pERK immunoreactive cells in lateral BLA (lBLA) and medial BLA/amygdaloid intermedullary grey (mBLA/IMG) of *WT* and *Nf1*$^{+/-}$ mice.

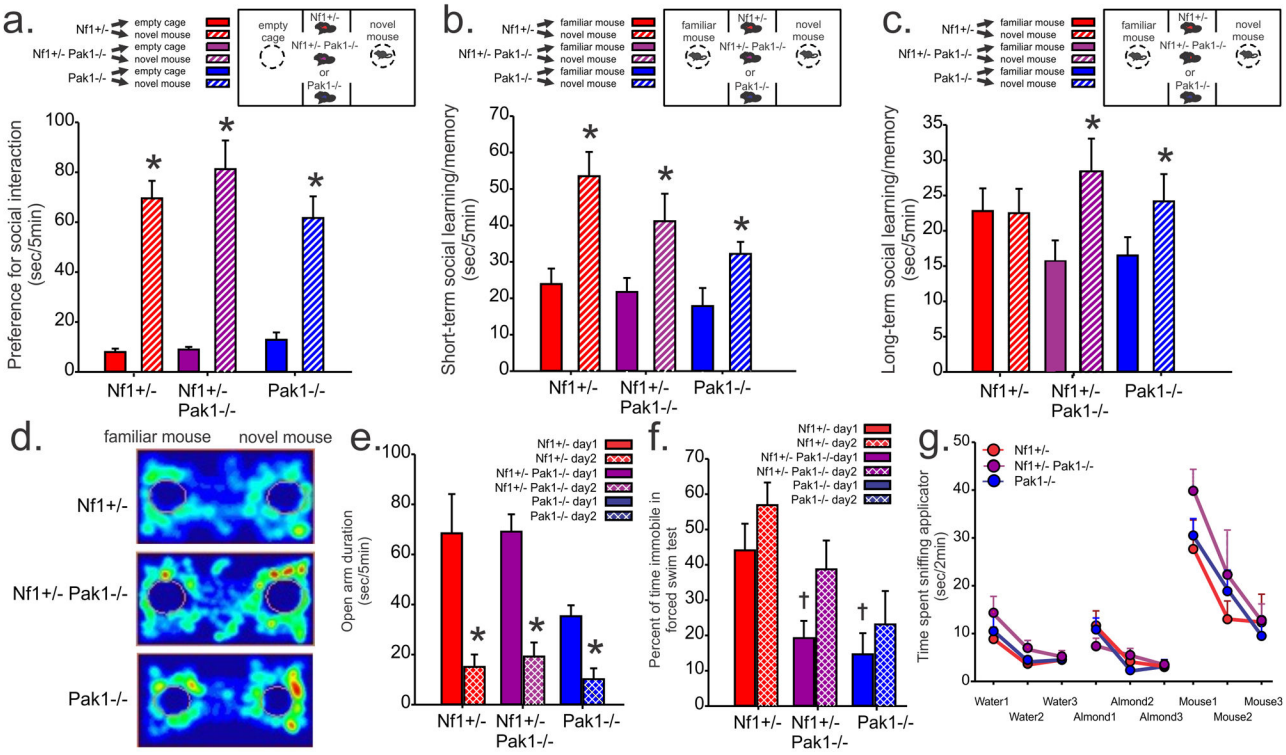

Figure 2. Deficits in long-term social learning in *Nf1*$^{+/-}$ mice are rescued in *Nf1*$^{+/-}$/*Pak1*$^{-/-}$ mice

Figure 2a–d depicts the time spent sniffing wire cages containing "stimulus" mice in a three-chambered apparatus (refer to insets that illustrate the orientation of cages and when cages were empty or contained a novel or familiar mouse; *Nf1*$^{+/-}$; *Nf1*$^{+/-}$/*Pak1*$^{-/-}$; *Pak1*$^{-/-}$). Similar to our previous findings, no differences were detected between strains in (**a**) preference for social interaction or (**b**) short-term social learning. (**c**) Unlike *Nf1*$^{+/-}$ mice, *Nf1*$^{+/-}$/*Pak1*$^{-/-}$ showed significant preference for social novelty or restored long-term social learning (24 hrs. following exposure to "test" mouse). **(d)** represents comprehensive heat maps of time spent in each region. No differences were observed in (**e**) anxiety as measured by elevated plus maze, **(f)** depression-associated behavior, or (**g**) olfactory habituation. Graphs depict mean ± SEM for *Nf1*$^{+/-}$ (red), *Nf1*$^{+/-}$/*Pak1*$^{-/-}$ (purple), and *Pak1*$^{-/-}$ (blue) mice. **P* < 0.05.

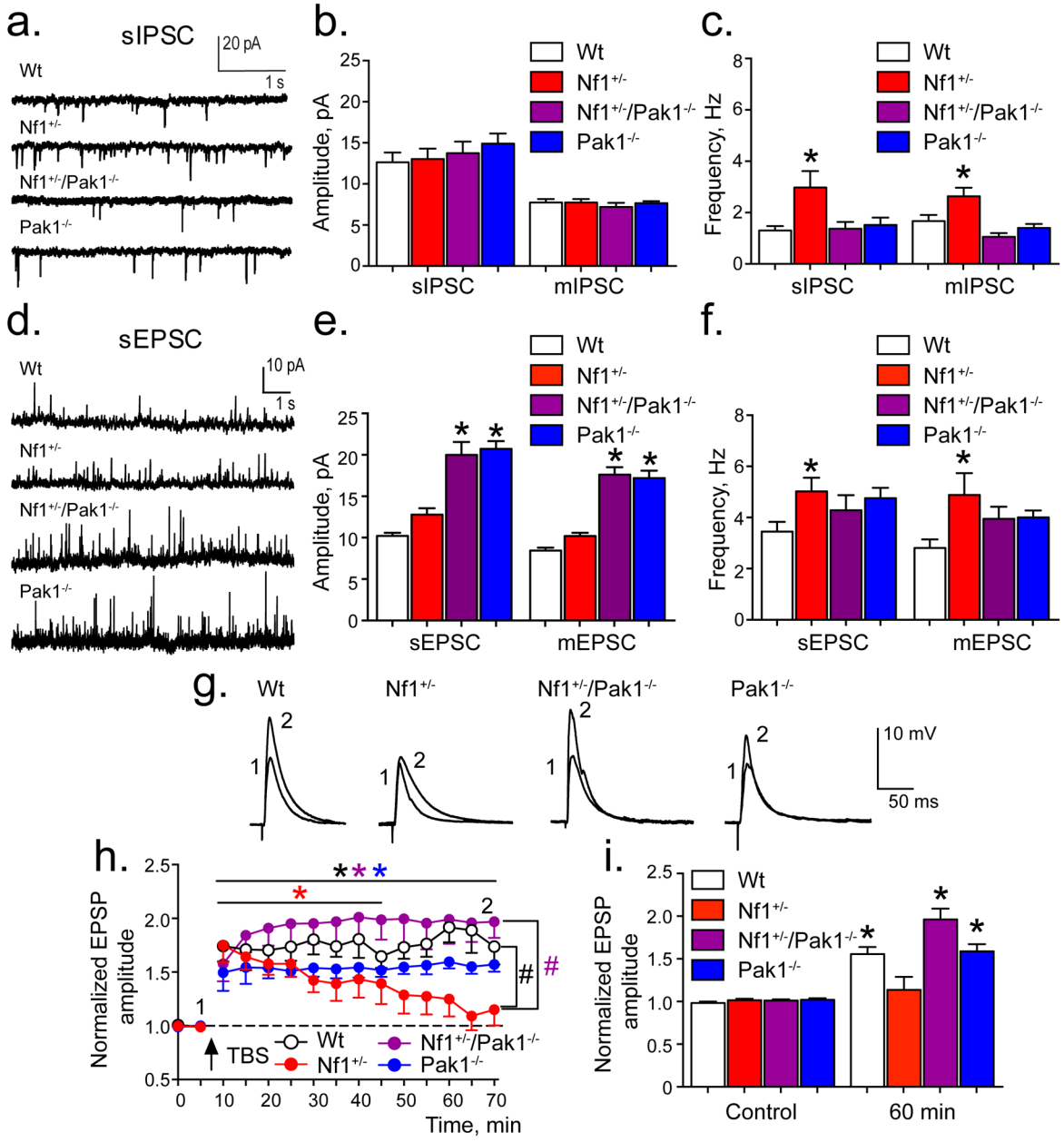

Figure 3. *Nf1*$^{+/-}$ mice exhibit elevated GABA and glutamate tones and significant LTP deficits in the BLA. Co-deletion of the *Pak1* gene restores GABA neurotransmission and LTP in the BLA

(**a**) Representative electrophysiological recordings of sIPSC at holding potential of −55 mV from pyramidal neurons of the BLA of *WT*, *Nf1*$^{+/-}$, *Nf1*$^{+/-}$/*Pak1*$^{+/+}$ and *Pak1*$^{+/+}$ mice. **(b,c)** Neurons from *Nf1*$^{+/-}$ mice exhibit no differences in sIPSC and mIPSC amplitude, but have significantly higher sIPSC and mIPSC frequency in the BLA compared to *WT* (n = 11,11,14,14). **(d)** The representative recordings of isolated sEPSC and mEPSC from BLA pyramidal neurons at a holding potential of −60 mV in *WT*, *Nf1*$^{+/-}$, *Nf1*$^{+/-}$/*Pak1*$^{-/-}$, *Pak1*$^{-/-}$ mice. **(e,f)** Compared to *WT*, *Nf1*$^{+/-}$ mice showed significant increases in frequency of sEPSCs (n = 17,14,16,19) and mEPSCs (n = 17,15,13,15), but not amplitude of

sEPSCs and mEPSCs. *Nf1*$^{+/-}$*/Pak1*$^{-/-}$ and *Pak1*$^{-/-}$ mice demonstrated significant increase of sEPSC and mEPSC amplitude **(e)** and no significant changes in sEPSC and mEPSC frequency **(f)** compared to *WT* mice. *represents $P \leq 0.05$ compared to control. **(g)** Representative traces of EPSPs before (1) and 60 min after (2) TBS stimulation of thalamic inputs to the BLA at holding potential of −70 mV. **(h)** Time course of averaged evoked EPSCs in response to stimulation of thalamic afferents in all neurons recorded from WT (white circle), N*f1*$^{+/-}$ (red), *Nf1*$^{+/-}$*/Pak1*$^{-/-}$ (purple) and *Pak1*$^{-/-}$ (blue) mice, respectively. TBS-LTP amplitude was significantly lower in *Nf1*$^{+/-}$, compared to *WT* mice. The significant depression of LTP was restored by co-deletion of *Pak1*. Data represent the mean ± SEM for each group; *represents $P < 0.05$ for comparison within groups. $^{\#}$(black) represents $P < 0.05$ *Nf1*$^{+/-}$ vs *WT* mice, $^{\#}$(purple) - *Nf1*$^{+/-}$ vs *Nf1*$^{+/-}$*/Pak1*$^{-/-}$ mice. **(i)** The summary graph showing the group data for the effects of tetanic stimulation protocol on EPSP amplitude before (Control) and 60 min after stimulation in *WT* (white, n = 7), *Nf1*$^{+/-}$ (red, n = 12), *Nf1*$^{+/-}$*/Pak1*$^{-/-}$ (purple, n = 8), and *Pak1*$^{-/-}$ (blue, n = 5) mice. Graphs depict mean ± SEM for each group. *represents $P < 0.05$ compared to control..

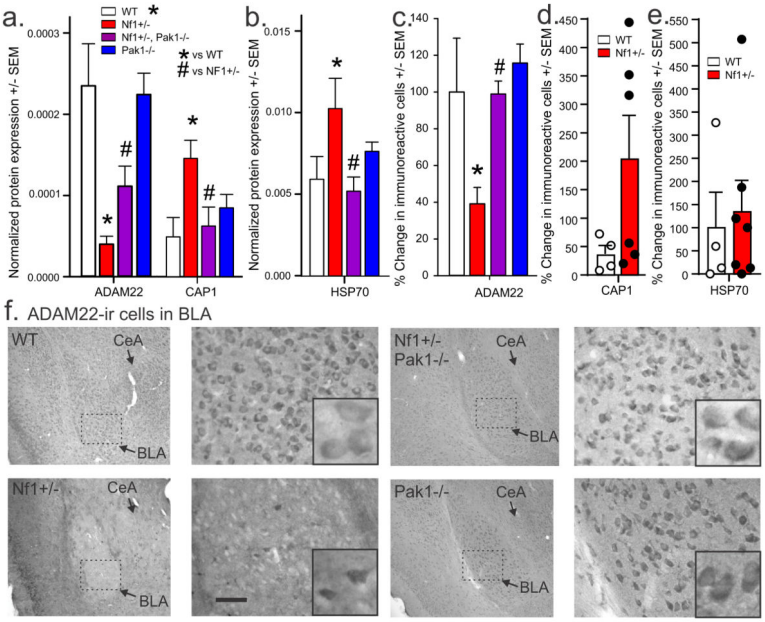

Figure 4. Reductions in ADAM22 levels and number of immunopositive cells seen in the BLA of *Nf1*$^{+/-}$ mice were rescued by the co-deletion of *Pak1* gene

Graphs in **(a–b)** represents normalized protein expression of ADAM22, CAP1 and HSP70 in the BLA of *WT*, *Nf1*$^{+/-}$, *Nf1*$^{+/-}$/*Pak1*$^{-/-}$, and *Pak1*$^{-/-}$ mice. Graphs in **(d–f)** respectively represents the number of ADAM22, CAP1 and HSP70 immunoreactive (ir) cells in the BLA of *WT* and *Nf1*$^{+/-}$ mice (and additional *Nf1*$^{+/-}$/*Pak1*$^{-/-}$, and *Pak1*$^{-/-}$ mice for only ADAM22). Bars represent the mean and error bars represent the standard error of the mean. * and # in **a–c** respectively indicate $P < 0.05$. **(f)** contains low (left) and high (right) photomicrographs of ADAM22-immunoreactive cells in the amygdala of *WT*, *Nf1*$^{+/-}$, *Nf1*$^{+/-}$/*Pak1*$^{-/-}$, and *Pak1*$^{-/-}$ mice. CeA and BLA are indicated with arrows in left row. Dashed lined box in left photomicrographs indicated where cells were counted and also where high magnification photomicrographs to right are taken. Scale bar for photomicrographs in left and right rows and inset are respectively, 25, 75 and 375 μm. See Suppl. Fig. 1b for a hypothetical illustration depicting glutamate and GABA regulation of normal EPSCs, LTP and IPSCs activity in *WT* mice, and how in *Nf1*$^{+/-}$ mice disruption of ADAM22 interrupts anchoring of AMPA receptors to the post-synaptic membrane and leads to non-sustainable LTP as demonstrated in Figure 3h. Similarly, increased expression of HSP70 could contribute to increases in pre-synaptic GABA release and increased frequency of IPSCs seen in Figure 3c. Abbreviations: BLA, basolateral amygdala; CeA, central amygdala.

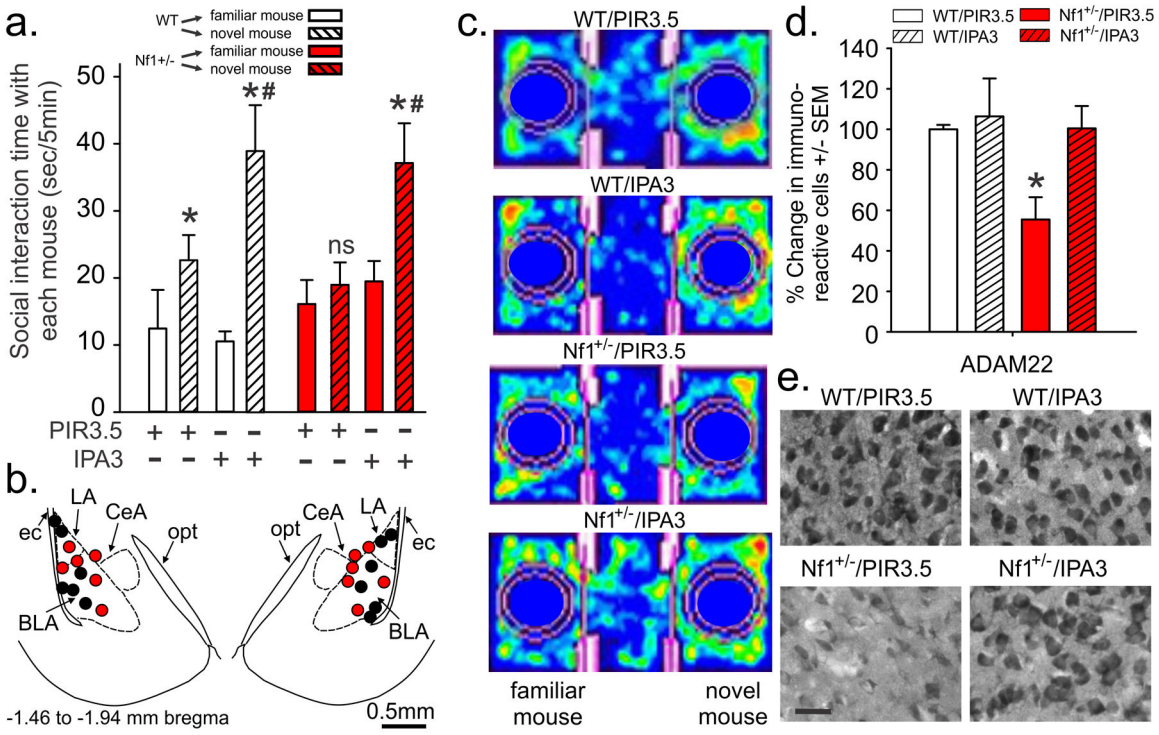

Figure 5. Bilateral injections of a PAK1 inhibitor IPA3 (and not the inactive enantiomer PIR3.5) into the BLA of *Nf1*$^{+/-}$ mice rescues their social learning deficits

(a) depicts the time spent in close proximity to either the novel or familiar mouse cage (≤ 2.5cm from wire cage) [* indicates a novel mouse preference, # indicates an enhanced social preference in *WT* mice, and a rescue of social preference in *Nf1*$^{+/-}$ mice, $P < 0.05$]. Graphs depict mean ± SEM. **(b)** is an illustration of a coronal mouse brain section (taken from Paxinos & Franklin stereotaxic atlas of the mouse brain, 3rd edition[38]) indicating the location of the injection sites (indicated by red circles) within the BLA from −1.46 to −1.94 mm bregma with a 0.5 mm scale bar at bottom right. Abbreviations: CeA, central amygdala; ec, external capsule; LA, lateral amygdala; opt, optic tract. **(c)** representative heat maps of time spent in each region with IPA3 groups spending more time near novel mouse cage. **(d)** Bar graph represents the number of ADAM22-immunoreactive (ir) cells in the BLA of *WT* and *Nf1*$^{+/-}$ mice treated with vehicle or IPA3 from crossover experiment from Fig. 5a–c. Bars represent the mean and error bars represent the standard error of the mean. *indicates a $P < 0.05$ versus all other groups. **(e)** contains photomicrographs of ADAM22-immunoreactive cells in the BLA of *WT, Nf1*$^{+/-}$ mice treated with vehicle or IPA3. Scale bar for photomicrograph is 25 μm.

Table 1

Protein expression differences (from 380 proteins screened) in the basolateral amygdala of *Nf1*$^{+/-}$ mice that were rescued by the co-deletion of *Pak1* gene (see also Fig. 4a–c for bar graphs)

Of the 380 proteins that were assessed in the BLA, there were an additional 70 that had significant differences in expression in *Nf1*$^{+/-}$ deficient mice compared to *WT* controls, but were not rescued (see Suppl. Table 1). Columns represent proteins showing full or partial rescue with *Pak1*$^{-/-}$ co-deletion with *Nf1*$^{+/-}$. Column 2 is the locus ID of each protein. Column 3 represents fold changes in protein expression in *Nf1*$^{+/-}$ mice compared to *WT* controls. Column 5 represents definitions for abbreviated proteins in column 1.

Protein	Locus ID	Fold-change	Description
‡ CAP1	P40124	3.05	Adenylate cyclase-associated protein 1
‡ HSP70	P63017	1.71	Heat shock protein 70
* † ADAM22	Q9R1V6	−6.17	ADAM metallopeptidase domain 22

‡, † *and* * symbols respectively indicated P < 0.05 using: ProteinQant; one-way ANOVA; or a two-way ANOVA [performed on log transformed protein expression data].